PROCEEDINGS OF THE YEREVAN STATE UNIVERSITY

Physical and Mathematical Sciences 2022, **56**(2), p. 66–73

P h y s i c s

IMAGING OF MICROWAVE NEAR-FIELD DISTRIBUTION OF GPS PATCH ANTENNA

Zh. A. BAGHDASARYAN[1,2]

[1] *Chair of Applied Electrodynamics and Modelling, YSU, Armenia*
[2] *Department of Physics, Sogang University, Seoul, Korea*

Microwave near-field distribution of the GPS patch antenna was visualized by a thermo-elastic optical indicator microscopy (TEOIM) technique at 1.575 GHz. Visualization of the antenna radiation is realized to describe the electromagnetic field intensity and distribution depending on the distance from the antenna surface and optical indicator. Experimental data was compared and confirmed with simulation results, which are in good agreement. Possible applications of the TEOIM system were discussed.

MSC2010: Primary: 00A79; Secondary: 74M05.

https://doi.org/10.46991/PYSU:A/2022.56.2.066

***Keywords*:** GPS antenna, near-field imaging, thermo-elastic optical indicator microscopy.

Introduction. The discovery of fast and easy antenna analysis methods in modern communication technology has a strategic significance [1–3]. Testing real antennas is fundamental to antenna theory and quite challenging. The most common and desired parameters for antenna measurement are radiation pattern, including antenna gain and efficiency, the impedance or voltage standing wave ratio (VSWR), the bandwidth, and the polarization. Different types of equipment are required for measuring the specific parameter for the antennas, which makes the tasks more difficult and complex. For instance, vector network analyzer (VNA) is one of the antenna's fundamental measuring devices that can measure the antenna's impedance. But in the case of the radiation pattern, gain and efficiency measurement require much more equipment like a reference antenna, power transmitter and receiver, positioning systems with anechoic chambers, etc.

With the growing technology as 5G, internet of things (IoT) and automotive systems, there is a necessity for new measurement techniques for RF applications, including near to far-field transformation, electromagnetic (EM) data acquisition systems, EM source reconstruction, etc. Many technologies have been developed

* E-mail: zhirayr.baghdasaryan@ysu.am

for antenna optimization and measurement based on specific requirements [4–8]. Thermo-elastic optical indicator microscopy (TEOIM) technique for antenna testing can provide different information related to the antenna radiation pattern, structural defects [9], and directivity; it can allow the evaluation of the radiated power and investigate how the field is distributed on the antenna surface and how it changes in the near region. The TEOIM may become an essential tool for engineers and researchers, and it can successfully be a supplement to existing measurement methods.

This article presents a GPS patch antenna investigation by a TEOIM. Note that each GPS satellite transmits data on the following frequencies L1 $(1575.42\ MHz)$, L2 $(1227.60\ MHz)$ and L5 $(1176.45\ MHz)$ [10]. The TEOIM is an optical visualization technique with non-reference antenna measurement. The microwave near-field (MWNF) distribution on the surface of the antenna structure was visualized at several distances. At the same time simulation model was created based on the actual GPS antenna structure to compare the results with experiments. We present an example demonstrating GPS antenna visualization, where TEOIM provides a comparable measurement performance to existing techniques and a capability of visualizing the MWNF distribution for various experimental conditions. A wide range of visualization, fast measurement throughput, and easy configuration setup are the main advantages of the TEOIM system. Especially for printed antennas, it can be an excellent method to investigate the antenna's performance, and understand how it operates near the PCB elements [11, 12], which is crucial in modern electronics and communication techniques.

Experimental Setup. IThe TEOIM technique uses a polarized light microscope method. Fig. 1 shows the experimental setup and antenna measurement configuration. Commercially available Indium-tin-oxide (ITO) glass with a 100 *nm* thin layer was used as an optical indicator. The light was emitted from the LED $(\lambda = 470\ nm)$ and was polarized circularly by passing through a linear polarizer (90º) and quarter waveplate (fast-axis 45°). The reflected light passed through the stressed glass changes the polarization from circular to elliptical due to the photo-elastic effect. In addition, the EM signal radiated by the patch antenna interacts with the optical indicator and heats ITO thin film. This heated ITO absorber is a creature of the mechanical stresses in the glass substrate. The CCD camera detects the linear birefringent (LB) distribution images by choosing the analyzer (linear polarizer sheet) orientation to be 0° or 45°. The detected heat distribution corresponds to the initial EM field distribution of the antenna. By solving the inverse problem of the mechanical stress formation, one can calculate the initial heat distribution causing those deformations with the custom image processing algorithms [13].

The RF signal was generated by a synthesized sweeper HP 83620A at the power of 0 *dBm*, amplified by a power amplifier ZHL-42W+ ("Mini-Circuit") up to 35*dBm*. RF devices and GPS patch antenna were connected by coaxial cables, as shown in Fig. 1. The antenna was placed close to an optical indicator and was held by a 3-axial stage. There, one axis was motorized by a motorized actuator Z812B ("Thorlabs") to change the distance between the antenna and optical indicator automatically.

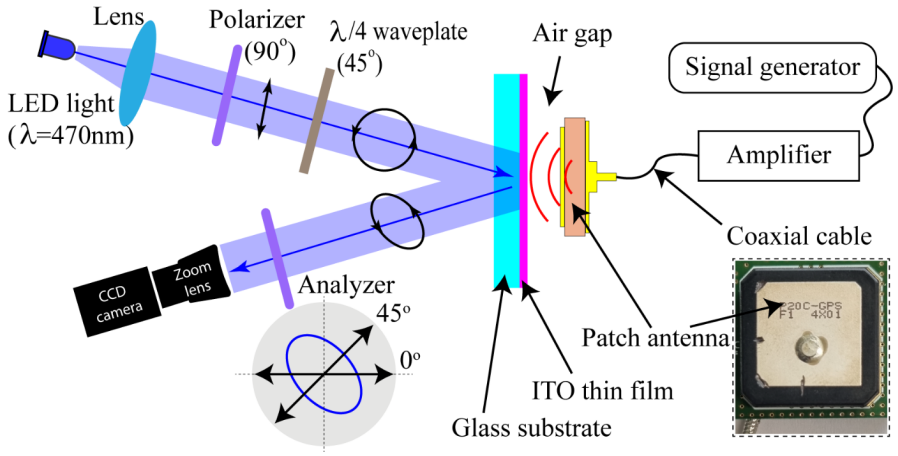

Fig. 1. Illustration of measurement principle of the TEOIM visualization system. Inset shows the photograph of the GPS patch antenna.

Simulation. Numerical analyses were conducted to show the GPS antenna's EM field distributions. The model is simulated by COMSOL Multiphysics software, where the simulation model consists "Electromagnetic Waves, Frequency Domain" physics interface. Fig. 2 (a) shows the 3D geometry of the GPS patch antenna in the simulation model. A rigid coaxial cable composed of Teflon ($\varepsilon_r = 2.1$) is attached to the bottom of the dielectric substrate, and the outer conductor of the coaxial cable is connected to the ground plane. The inner conductor pin of the cable is extended through the dielectric part of the substrate and connected to the patch on the top surface. All metal parts, including the patch, ground plane, and inner and outer conductors of the coaxial cable are modeled as perfect electric conductors. The geometry of the patch antenna is designed based on the real GPS antenna, which was used as a device under test (DUT) for measurement by the TEOIM system. The patch antenna structure was shown in the top view of the designed model (Fig. 2 (b)). The real value of the substrate dielectric permittivity is unknown for the antenna used in the experiment. However, due to numerical analysis, the dielectric permittivity of the substrate was estimated to be ε_r=35. A coaxial lumped port is used to excite the antenna with the reference impedance of 50 Ω with a coaxial probe feed. Fig. 2 (c) shows the simulated radiation plot of E- and H- planes in terms of far-field gain (dBi) at the resonant frequency of the GPS patch antenna (1.575 GHz). From that graph it is clear that the proposed antenna is used to enhance the gain and directional capabilities. Fig. 2 (d) shows radiation's directivity, which is evaluated from a 3D far-field pattern. The pattern is directed to the positive z-direction due to the antenna's ground plane. The calculated maximum directivity value for the GPS patch antenna is around 3.65 dB. However, the truncated patch antenna shows the radiating fields confined at each patch corner. The antenna performs almost identically at every azimuthal angle in terms of the field intensity magnitude.

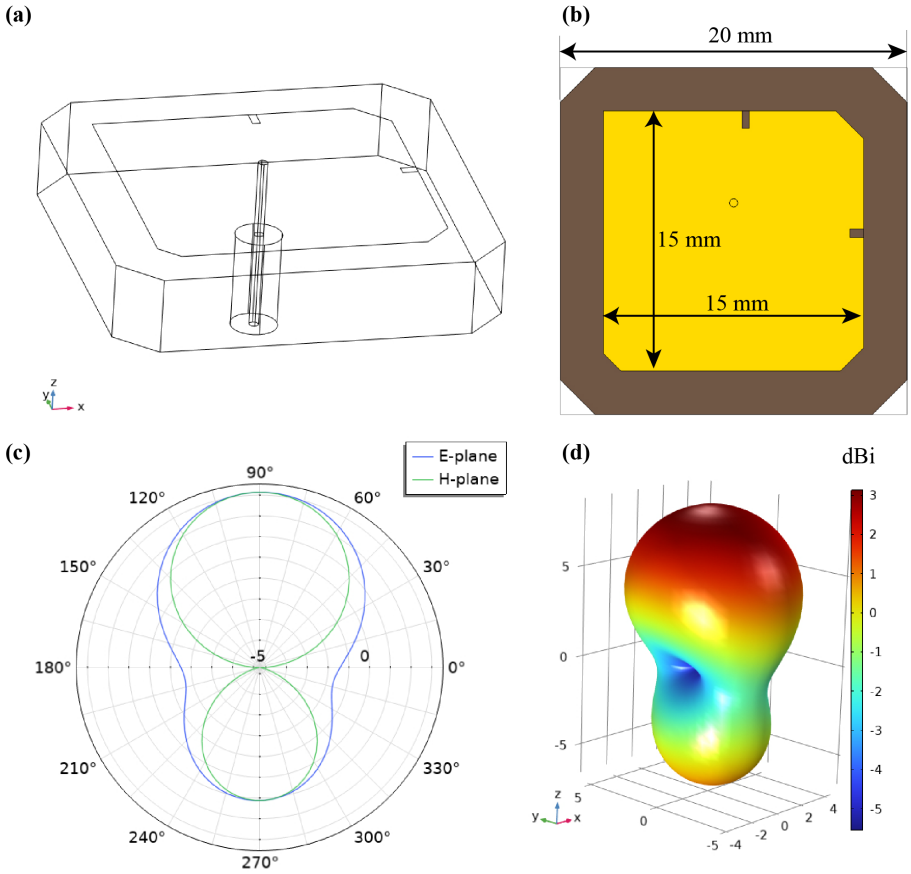

Fig. 2. (a) 3D geometry of the GPS patch antenna in the simulation model. (b) Top view of the patch antenna. (c) Far-field radiation pattern (gain in dBi) at E-plane and H-plane. (d) 3D radiation pattern for far-field gain (dBi).

Results and Discussion. The optical indicator of the TEOIM system consists of an ITO thin and uniform metallic film deposited on the glass substrate, which can strongly interact with the EM field. Due to this interaction, the metal becomes heated due to EM energy.

Depending on the lossy property of the indicator, it can be heated by a magnetic or electric field. It is known that the microwave magnetic field heats a conductive thin film by the inductive heating process because resistive losses dominate in metallic and high conductive materials [14–16]. Therefore, the thin metal of the OI will be heated depending on the magnetic MWNF spatial distribution. The distance between the indicator and the DUT was sequentially increased during the visualization process. Fig. 3 (a) shows experimental results related to in-plane magnetic MWNF distributions at 1.575GHz for 0, 2, 4, and 6 mm from left to right. As we can see from the images, by increasing de distance between the indicator and DUT, the average intensity of the Magnetic MWNF distribution decreases and localized field distribution from the left and right edges shift to the center of the patch surface.

The inner highlighted contour shows the location of the patch antenna, and the outer highlighted contour displays the shape of the dielectric substrate of the antenna. Fig. 3 (b) illustrates the simulation results corresponding to Fig. 3 (a) for magnetic MWNF distributions for different distances. Distributed fields for simulation and experiment are in good agreement, and the decreasing intensity behavior also shows a similar tendency. Fig. 3 (b) illustrates the simulation results corresponding to Fig. 3 (a) for magnetic MWNF distributions for different distances. Distributed fields for simulation and experiment are in good agreement, and the decreasing intensity behavior also shows a similar tendency.

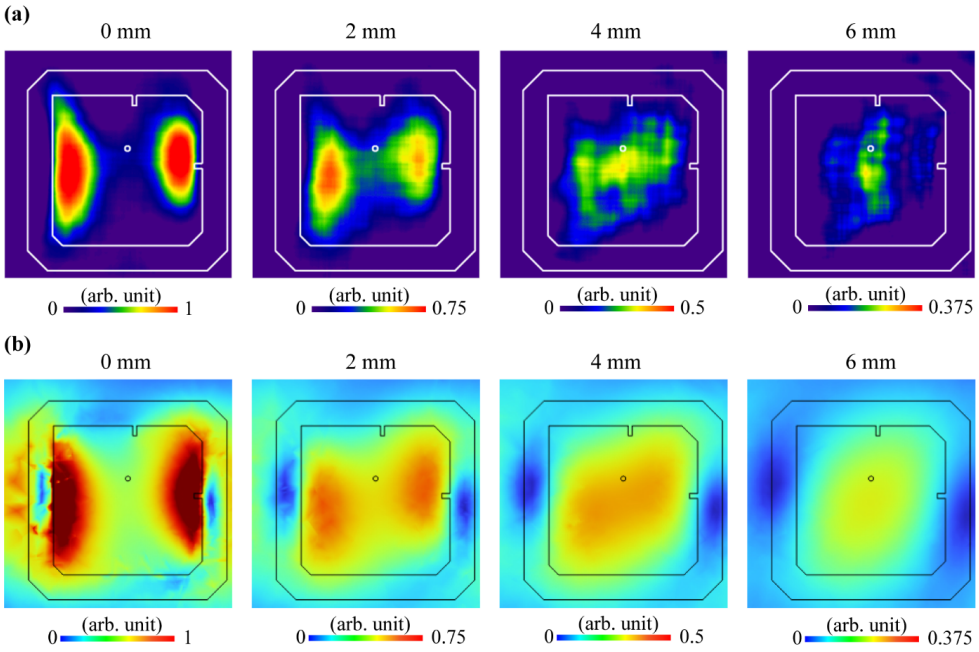

Fig. 3. (a) Experimental and (b) simulated visualization of the in-plane magnetic MWNF distribution at 1.575 GHz corresponding to the distance between indicator and antenna surface $(0,\ 2,\ 4,\ 6\ mm)$.

In addition, Fig. 4 (a) shows the S_{11}-parameter for actual and simulated GPS patch antennas. The obtained date shows that the resonant signal of antenna at 1.575 GHz is $-17\ dB$ for simulation and $-10\ dB$ for measurement, which is sufficient for GPS applications. At $-10\ dB$, the S_{11} bandwidth is about 30 MHz for the simulation model, but for the actual GPS antenna, 30 MHz bandwidth is obtained at $-8\ dB$. By increasing the distance of the GPS antenna and optical indicator, the detected average field intensity decreases as expected, and the decreasing tendency for simulation and measurement is illustrated in Fig. 4 (b). The values in Fig. 4 (b) were calculated based on the average intensity of the field distribution illustrated in Fig. 3. This optical method of antenna measurement in the future can increase antenna design applications and positively impact manufacturing and monitoring due to its experimental agility.

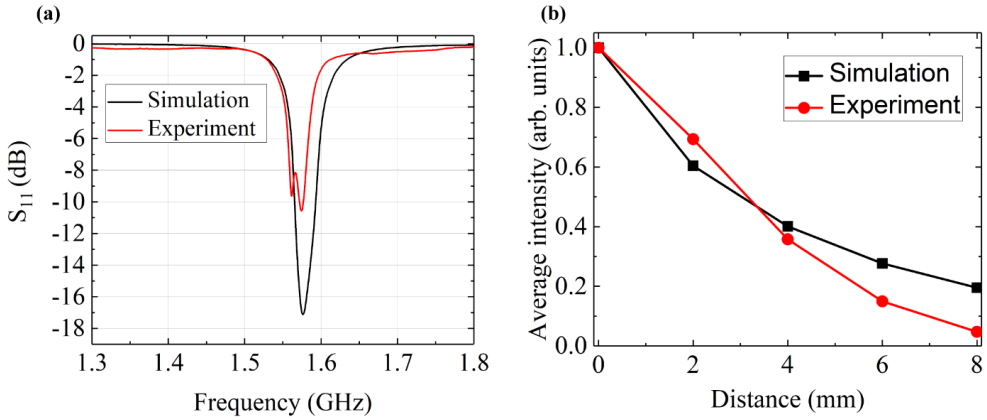

Fig. 4. (a) S_{11}-parameter of the patch antenna. (b) The average intensity of the MWNF distribution vs. the distance between the antenna surface and the optical indicator.

Conclusion. The MWNF distribution in the near region of the GPS patch antenna was visualized by a TEOIM technique. According to experimental and simulation results, this visualization method can effectively analyze the antenna's parameters by providing information related to a radiation pattern, radiated power, and structural defects. Magnetic MWNF distribution intensity depending on the distance between the optical indicator and the antenna was evaluated and compared with the simulation results. They both show a similar decreasing tendency. This antenna characterization method can be an atractive tool in the field of antenna design and measurements.

We thank Prof. A. Babajanyan and Prof. K. Lee for valuable discussions and support during the research.

Received 08.06.2022
Reviewed 08.07.2022
Accepted 18.07.2022

REFERENCES

1. Fan W., Kyosti P., et al. Over-the-air Radiated Testing of Millimeter-wave Beam-steerable Devices in a Cost-effective Measurement Setup. *IEEE Commun. Mag.* **56** (2018), 64–71. https://doi.org/10.1109/MCOM.2018.1701006
2. Xue W., Chen X., et al. Statistical Analysis of Antenna Efficiency Measurements with Non-Reference Antenna Methods in a Reverberation Chamber. *IEEE Access* **8** (2020), 113967–113980. https://doi.org/10.1109/ACCESS.2020.3003530

3. Pozar D.M., Kaufman B. Comparison of Three Methods for the Measurement of Printed Antenna Efficiency. *IEEE Trans. Antennas Propag.* **36** (1988), 136–139. https://doi.org/10.1109/8.1084
4. Luo Q., Zhou Y., et al. Rapid Test Method for Multi-beam Profile of Phased Array Antennas. *Sensors* **22** (2022). https://doi.org/10.3390/s22010047
5. Coq Le L., Mézières N., et al. Some Contributions for Antenna 3D far Field Characterization at Terahertz. *Sensors* **21** (2021), 1–11. https://doi.org/10.3390/s21041438
6. Rodríguez Varela F., López Morales M.J., et al. Multi-Probe Measurement System Based on Single-Cut Transformation for Fast Testing of Linear Arrays. *Sensors* **21** (2021), 1744. https://doi.org/10.3390/s21051744
7. Capozzoli A., Curcio C., Liseno A. Different Metrics for Singular Value Optimization in Near-field Antenna Characterization. *Sensors* **21** (2021), 1–15. https://doi.org/10.3390/s21062122
8. D'agostino F., Ferrara F., et al. Reconstruction of the Far-field Pattern of Volumetric Auts from a Reduced Set of Near-field Samples Collected along a Planar Spiral with a Uniform Step. *Sensors* **21** (2021), 1–13. https://doi.org/10.3390/s21051644
9. Arakelyan S., Lee H., et al. Antenna Investigation by a Thermoelastic Optical Indicator Microscope: Defects Measurement and 3D Visualization of Electromagnetic Fields. *IEEE Antennas Propag. Mag.* **61** (2019), 27–31. https://doi.org/10.1109/MAP.2019.2895667
10. Doust E.G., Clénet M., et al. An Aperture-coupled Circularly Polarized Stacked Microstrip Antenna for GPS Frequency Bands L1, L2, and L5. *IEEE Int. Symp. Antennas Propag. Usn. Natl. Radio Sci. Meet. APSURSI* **1** (2008), 25–28. https://doi.org/10.1109/APS.2008.4619440
11. Zhang F., Qiao N., Li J. A PCB Photoelectric Image Edge Information Detection Method. *Optik (Stuttg)* **144** (2017), 642–646. https://doi.org/10.1016/j.ijleo.2017.07.002
12. Kacprzak D., Taniguchi T., et al. Novel Eddy Current Testing Sensor for the Inspection of Printed Circuit Boards. *IEEE Trans. Magn.* **37** (2001), 2010–2012. https://doi.org/10.1109/20.951037
13. Lee H., Arakelyan S., et al. Temperature and Microwave Near Field Imaging by Thermoelastic Optical Indicator Microscopy. *Sci. Rep.* **6** (2016), 1–11. https://doi.org/10.1038/srep39696
14. Yoshikawa N. Fundamentals and Applications of Microwave Heating of Metals. *J. Microw. Power Electromagn. Energy* **44** (2010), 4–13. https://doi.org/10.1080/08327823.2010.11689772
15. Bosman H., Lau Y.Y., Gilgenbach R.M. Microwave Absorption on a Thin Film. *Appl. Phys. Lett.* **82** (2003), 1353–1355. https://doi.org/10.1063/1.1556969
16. Lee H., Baghdasaryan Z., et al. Detection of a Conductive Object Embedded in an Optically Opaque Dielectric Medium by the Thermo-Elastic Optical Indicator Microscopy. *IEEE Access* **7** (2019), 46084–46091. https://doi.org/10.1109/ACCESS.2019.2908885

Ժ. Ա. ԲԱՂԴԱՍԱՐՅԱՆ

GPS ՓԱՉ ԱՆՏԵՆԱՅԻ ՄԻԿՐՈԱԼԻՔԱՅԻՆ ՄՈՏԱԿԱ-ԴԱՇՏԻ ԲԱՇԽՎԱԾՈՒԹՅԱՆ ԱՐՏԱՊԱՏԿԵՐՈՒՄԸ

Ջերմաառաձգական օպտիկական ինդիկատորով մանրադիտակի (ՋԱՕԻՄ) միջոցով արտապատկերվել է GPS փաչ անտենայի միկրոալիքային մոտակա-դաշտի բաշխվածությունը 1,575 GHz հաճախության դեպքում: Էլեկտրամագնիսական դաշտի ինտենսիվության և բաշխվածության կախվածությունը անտենայի մակերևույթիի և օպտիկական ինդիկատորի միջև եղած հեռավորությունից բնութագրելու նպատակով իրականացվել է անտենայի ճառագայթման արտապատկերում: Փորձարարական տվյալները համեմատվել և հաստատվել են համակարգչային մոդելավորման արդյունքներով: Քննարկվել են ՋԱՕԻՄ արտապատկերման համակարգի հնարավոր կիրառությունները:

Ж. А. БАГДАСАРЯН

ВИЗУАЛИЗАЦИЯ МИКРОВОЛНОВОГО РАСПРЕДЕЛЕНИЯ ПАТЧ-АНТЕННЫ GPS В БЛИЖНЕЙ ЗОНЕ

Распределение микроволнового поля в ближней зоне патч-антенны GPS было визуализировано с помощью термоупругого оптического индикаторного микроскопа (ТУОИМ) на частоте 1,575 *ГГц*. Оценивалась визуализация излучения антенны для различных интенсивности и распределения электромагнитного поля в зависимости от расстояния между поверхностью антенны и оптическим индикатором. Экспериментальные результаты были сопоставлены и подтверждены результатами моделирования. Обсуждаются возможные применения системы ТУОИМ.